Motion Analyses in Modeling of Flow and Contaminant in Cleanrooms: A Review

Maysam Saidi[1,*] , Jaber Eslami[2]

[1] Mechanical Engineering Department, Faculty of Engineering, Razi University, Kermanshah, Iran
2 Mechanical Engineering Department, Amirkabir University of Technology, Tehran, Iran

ACCEPTED MANUSCRIPT

Abstract

The motion effect on the contaminant dispersion is a key parameter in cleanrooms. This parameter is ignored in many experimental and numerical studies because of its complexities, but could cause errors in the obtained results. In real situations, particularly in the isolating rooms and cleanrooms, the motion that is usually caused by the human moving and doors opening and closing leads to considerable flow changes that require attention. The present study aimed to explore studies that noticed and studied different aspects of the subject and to summarize the areas with priority for further investigation. Modeling the problem using experimental and numerical approaches requires steps and settings that are described in the experimental and numerical sections. The motion analysis is divided into two sections of human and door motions, covering the key findings of previous and recent publications, and concluding the required future studies. The results of approximately fifty published studies have revealed important findings related to cleanroom class degradation, temperature gradient reduction, increased contamination and secondary flow depth, and particle settlement on patients. These studies have shown that the ventilation system may need to be redesigned. Furthermore, it is crucial to consider the motion in both experimental and numerical studies based on the application. Additional research is necessary to further understand these findings.

Keywords: Cleanroom, Door motion, Human motion, Modeling

[*] Corresponding author, *Assistant Professor, Razi University, Kermanshah, Iran 6714414971, Phone: +98-83-34343013, Fax: +98-83-34343010, Email: msaidi@razi.ac.ir*

1. Introduction

Environmental pollution is an important issue in various places, causing a variety of problems. The parameters affecting contaminant distribution are an interesting subject to study. Various particle sizes are observed in the atmosphere. Airborne particulate matters (PM) are small enough to be suspended. They may be mixtures of organic and inorganic substances with different physical properties, chemical compositions, mass concentrations, and size distributions. Particulate matter with an aerodynamic diameter greater than 2.5 microns is assumed as coarse particles, while particles smaller than 2.5 microns are fine particles [1]. Health is an important topic in this categorization. Viruses such as COVID-19 and SARS need airborne particles or droplets to be distributed.

Airborne particulate matter has different sizes, shapes, and compositions. The smallest ultrafine particles were produced by nucleation and condensation, generally from combustion releases. Ultrafine particles are characteristically unstable and grow through coagulation and condensation to larger growth particles with a diameter of 0.1-1 microns which above half of the particle mass in air is in this range. Particles greater than 1-2 microns generally have different backgrounds and compositions and are generated mainly by mechanical processes, such as wind or abrasion. These coarse particles can vary in size, up to 100 μm, and greater particles will settle down shortly and are not known as airborne [2].

Particulate matter exposure in humans increases morbidity and mortality. Substantial research has explored the potential biological mechanisms or pathophysiological pathways that connect particulate matter exposure to cardiopulmonary disease and death [3]. There are various studies on the effect of fine particle ($PM_{2.5}$) exposure on human health in comparison to coarse particles ($PM_{2.5-10}$) to understand the role of long and short exposure in morbidity and mortality due to respiratory diseases rather than on cardiovascular diseases [4]. A study in 205 cities showed

ACCEPTED MANUSCRIPT

that a 10 μg/m3 increase in $PM_{2.5-10}$ concentration increased the risk of total (0.51%), cardiovascular (0.43%), and respiratory (0.41%) mortality [5].

Airflow patterns, temperature, pressure, humidity, electrostatic discharge, gaseous contamination, sound, and vibration are among the most important factors that can be controlled under ambient conditions. The history of controlling air in hospital spaces has returned to first-century Roman military hospitals. Over the centuries, hospitals have been large, open halls that were well-heated, and ventilated. In addition, manufacturers require special contamination-controlled rooms. Manufacturers of precision military products were among the first users of ultra-clean rooms, white rooms, or cleanrooms [6]. World War II was known as the early use of ventilation in cleanrooms for operating rooms and missile manufacturing industries [7]. The notion that Western Electric's "dust-free" room, constructed in 1955, was an inaugural production cleanroom, has been contended by some. This room, which was engineered with filters that were 99.95% efficient and featured positive pressurization, was a bold achievement in cleanroom technology. However, others contend that the Olmsted Air Force Base in Pennsylvania or the U.S. Navy's North Island Naval Air Station in San Diego was the site of the first cleanroom installation [8].

The lack of self-cleaning capabilities and inadequate ventilation systems in cleanrooms during the mid-20^{th} century were significant challenges. Continuous cleaning by personnel was necessary to maintain a desired level of cleanliness. The invention of the laminar flow concept of ventilation by physicist Whitfield at Sandia Laboratories while working with the U.S. Atomic Energy Commission marked one of the first successful applications of this concept [9]. The maintenance of ancient buildings requires attention worldwide. Those with high traditional values have been destroyed progressively, for example, paintings in open tombs because of bioaerosol particle contamination by walking visitors [10].

ACCEPTED MANUSCRIPT

Operating rooms in hospitals require special attention for flow and particle distribution. An observational study of 28 surgeries (total time of 65.5 h) showed 23 door openings per hour, of which 23.5% were passage of external personnel. Door-opening durations were independent, but its frequency was dependent on the surgery type. They also found a noteworthy gap between the hold-open time and the period spent by the user to move across the door, which suggests that the door should be automatically closed after it is cleared [11].

Door operations and human passage led to air mixing across the cleanroom door. The door operation eliminates and even reverses pressurization across the door [12]. Operating room ventilation performance is influenced by several factors, including heat loads and obstacles, such as apparatus, people, and operating lamps. Door opening and human motion have been stated to harm the cleanliness and ventilation effectiveness of the operating room. In some aspects, such as the positive impact of appropriate staff work practices or the useful effect of protective clothing to limit particle distribution, the findings are straightforward. However, precise laboratory measurements and advanced computational predictions are essential to clarify these controversies in some subjects. For example, several studies have suggested laminar airflow ventilation, while others have reported a greater surgical site infection (SSI) rate in the existence of laminar airflow systems [13].

There are different standards used in cleanroom designs and operation. Maximum permitted total particle concentration are used to classify cleanroom types. While ISO classifies 9 Classes (1 to 9) in ISO14644-1 standard, European GMP-PIC/S standard uses 4 Classes (A, B, C, D). GMP classification considers in rest and in operation situations which the second one permits more particle number in its classes of B and C. Human motion and door opening and closing could alter the class and should be considered. For example, Shao et al. [14] evaluated the impact of human movement passing a door on short-term contamination in a cleanroom. While the initial steady concentration of 0.5 and 1 μm particles in the cleanroom was within the range

ACCEPTED MANUSCRIPT

of Classes 6 to 7, as defined by ISO 14644-1, with counts ranging from 18,519 to 100,482 in m^3, for doorway flow rate of 210 L/s (air speed of 0.11 m/s), the overall cleanroom environment was degraded to ISO Class 8 within a short period of time. However, there are different parameters affecting cleanroom class which needs to be studied.

The importance of health has been emphasized in different studies on air quality and human breathing. For example, in-flight transmission leads to the worldwide distribution of infectious diseases, including tuberculosis, influenza, measles, mumps, and SARS [15].

Moving human bodies in different places, such as airlines, operating rooms, isolation rooms, offices, and residential kitchens, generates local airflow, which promotes the distribution of the contaminants. Thus, the local flow formed from human motion on indoor air quality should be noticed. Although limited experiments have been conducted on human motion because of the complex measuring point arrangements, control of accurate experimental conditions, and expenses of experimental facilities, rising investigations have focused on numerical modeling of induced flows by object motions [16].

Experimental measurements and computational fluid dynamics (CFD) are two common approaches to study the flow and contaminant distribution. Each has its advantages and disadvantages. Experiments usually require fewer assumptions but further expense; thus, CFD usually is more efficient due to the progress in numerical methods and hardware facilities.

In recent years, the design of cleanrooms and control of airborne particles for diverse applications has garnered significant attention in both experimental and numerical studies. Motion including human and door alters the flow field and affect the contaminations in cleanroom which is crucial in many applications. This paper commences with a brief historical overview in the Introduction, emphasizing the pivotal role of motion in contemporary research. Subsequently, a concise summary of experimental and numerical techniques is presented,

ACCEPTED MANUSCRIPT

followed by a thorough examination of studies categorized into two areas of human and door motions as depicted schematically in Figure 1.

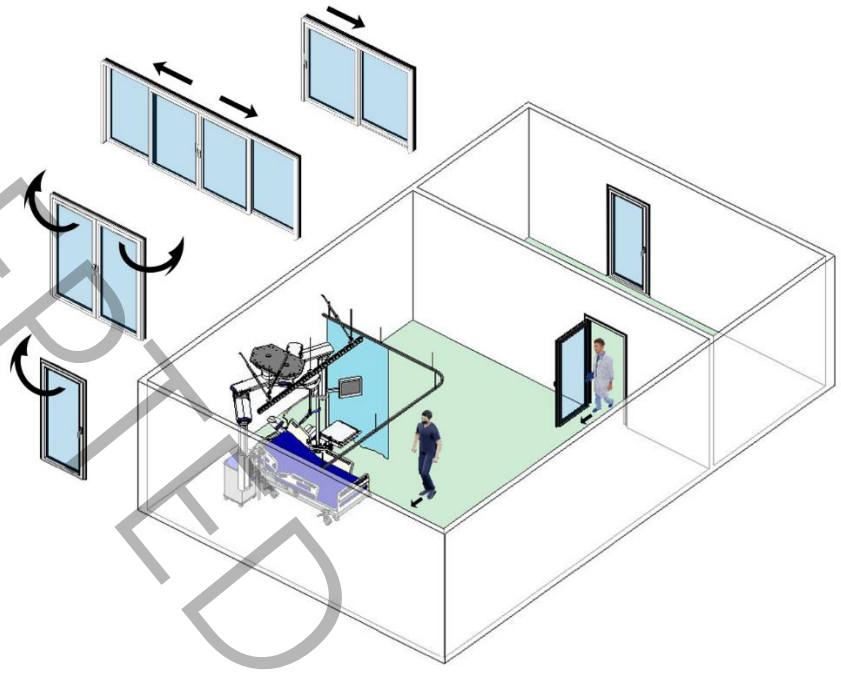

Fig. 1 A schematic of a ventilated room with door and human motions

2. Experimental Description

The rooms in the cleanroom literature are divided into three categories: bubble, sink, and cascade. The bubble model has a positive pressure, the supply air is greater than the exhaust, and extra flow exits from the door gaps. In contrast, the sink model has negative pressure, and air enters from the outside to the inside. The cascade model is typically between two bubble and sink rooms, receives air from one room, and delivers it to the other. The pressure difference between adjacent rooms is usually assumed to be 0, 2.5, 5, 7.5, 10, 12.5, 15, 20, 25, 37.5, and rarely, 50 Pa.

There are two strategies for assuming real or small-scale geometry. In small-scale studies, the similarity condition is an important issue, and the Reynolds number is typically checked. For this reason, substituting air with water is an approach used in some small-scale studies. Changing the motion speed and ACH are other parameters that require attention in such studies.

ACCEPTED MANUSCRIPT

Doors are divided into two categories: hinged (swing) and sliding, and each can be a single or double side. Human geometry is considered a moving object and can be assumed as a simple rectangular plate, cylindrical block, real manikin, or real human.

Air inlets and outlets to the room pass through the supply and exhaust or return diffusers in different forms, including swirls and perforated diffusers.

The inappropriate direction of air flows and the movement of air from the patient towards the healthcare worker and anteroom often led to the ineffective control of impurities. Despite the fact that an anteroom significantly reduces the leakage of infectious agents to the corridor, it does not prevent this completely when human move between the cleanroom and corridor. In order to improve the protection of cleanroom, it is crucial to focus on the air distribution and removal efficiency of impurities in both cleanroom and anterooms. Tracer gases are among methods to show the flow direction of air flow and leakage of contaminant between rooms. For example, Kokkonen et al. [17] found that when exhaust vents were located above the patient's head tracer gas was efficiently removed near its generation point which minimized the contaminant movement towards the healthcare working persons working area in an isolation room.

The measurement of the important parameters of pressure, temperature, humidity, and velocity requires attention in experimental procedures. The accuracy of the measuring devices and methods for reducing flow disturbance requires attention. Pitot tubes, vanes, ultrasound, and hot-wire anemometry are commonly used air velocity measurement methods.

Visualization of the flow field is an important phase of experiments. Image capturing and post-processing, with the distribution of smoke in air and ink in water, are among the most commonly used methods. Particle Image Velocimetry (PIV) is an applicable optical method that uses sufficiently small particles as tracers. Contamination can be assumed as a point source or the whole domain. Particle producers and counters are rarely used and expensive methods

ACCEPTED MANUSCRIPT

in contamination experimental studies that quantitatively report the size and concentration of particles. Usually, smoke and gas tracing are used to determine the contaminant distribution.

It should be noted that several experimental limitations make it challenging to obtain an accurate tracer gas concentration field. For instance, Saarinen et al. [18] utilized smoke visualization to observe the dispersion process; however, this technique lacks the ability to provide quantitative data to describe transient concentration levels. Poussou et al. [15] used Particle Image Velocimetry (PIV) and Planar Laser-Induced Fluorescence (PLIF) techniques to measure the flow field and contaminant transport. Although these methods are the best way to measure the concentration field, they can be extremely costly and difficult to implement. Another proposed approach involves the use of numerous tracer gas sensors. However, this option has a significant drawback, as the response time for the 95% concentration cannot be less than 2.0 s. If this method is used, only two or three data points can be collected before the door is closed. Several researchers have attempted to obtain the entire transient concentration field [19-21] measuring the total tracer gas mass at the final moment, resulting in only one quantitative value.

3. Numerical Description

The analysis of the numerical simulation sheds light on the weakening process of experiments and provides valuable insights for optimizing system design and operation. The governing equations for solving the flow field include mass, momentum, and energy equations, while for contaminant distribution, particle tracking is performed using the second law of Newton, gas tracing, or species transport equation. The boundary conditions used for the domain are divided into stationary and moving conditions. The stationary boundaries include the wall, inlet, and outlet as no-slip, velocity inlet, and pressure outlet, velocity outlet, or outflow, respectively. In

ACCEPTED MANUSCRIPT

cleanrooms, the escape for the openings and trap for the walls are assumed for the particle boundary condition.

The precise location for injecting particles is crucial and must be determined based on the specific application. The motion conditions, particle size, exhalation flow rate, social distancing, and respiratory model all impact the trajectory and ultimate deposition of the particles. Smaller droplets (around 3 μm) evaporate quickly and are profoundly influenced by thermal plumes, causing them to rise towards the ceiling with minimal deposition on individuals. On the other hand, larger droplets (60-175 μm) exhibit a higher deposition fraction on both the head and body of susceptible individuals [22]. Some studies assume an isothermal situation and neglect the temperature effects; however, the thermal plume effect is an important issue. The thermal condition is considered by solving the energy equation, and the buoyancy is considered by the Boussinesq approximation. Numerical studies in this area usually use the finite volume method for discretizing the domain, the SIMPLE algorithm for pressure-velocity decoupling, and turbulence models for equations closure. Using dynamic meshes, the integral form of the conservation equation for a general scalar φ, within an arbitrary control volume having a moving boundary, can be expressed as [23]:

$$\frac{d}{dt}\int_V \rho\varphi dV + \int_{\partial V} \rho\varphi(\vec{u}-\vec{u}_g).d\vec{A} = \int_{\partial V} \Gamma_{\varphi,eff}\nabla\varphi.d\vec{A} + \int_V S_\varphi dV \quad (1)$$

where ρ_f, $\vec{u}$, $\vec{u}_g$, S_φ, and $\Gamma_{\varphi,eff}$ are fluid density, fluid velocity, grid velocity, source term, and the diffusion coefficient, respectively. Table 1 lists commonly used governing equations in numerical studies with definition of φ and other relevant parameters.

Table 1 Parameters used in different governing equations [24]

Equation	φ	$\Gamma_{\varphi,eff}$	S_φ
Continuity	*1*	*0*	*0*
Momentum	$\vec{u}$	μ_{eff}	$-\nabla p-\rho_0\beta(T-T_0)\vec{g}$
Energy	*H*	λ_{eff}/C_P	*0*
Contaminant	*C*	ρD_{eff}	*0*

ACCEPTED MANUSCRIPT

Turbulent kinetic energy	k	μ_{eff}/σ_k	$P_k + G_b - \rho\varepsilon$
Turbulent kinetic energy dissipation rate	ε	$\mu_{eff}/\sigma_\varepsilon$	$\varepsilon(C_1 P_k - C_2\varepsilon + C_3 G_b)/k$

where:

$H = C_P(T - T_{ref})$ $\quad \mu_{eff} = \mu + \mu_t$ $\quad C_1 = 1.44$ $\quad \sigma_k = 1.0$

$P_k = \mu_t(U_{ij} + U_{ji})U_{ij}$ $\quad \lambda_{eff} = \lambda + \lambda_t$ $\quad C_2 = 1.92$ $\quad \sigma_\varepsilon = 1.3$

$G_b = \beta g_i \frac{\mu_t}{\mathrm{Pr}_t}\frac{\partial T}{\partial x_i}$ $\quad \lambda_t = C_P\mu_t / \mathrm{Pr}_t$ $\quad C_3 = C_1 \tanh(v/u)$ $\quad \mathrm{Pr}_t = 0.85$

$\mu_t = C_\mu \rho k^2/\varepsilon$ $\quad D_{eff} = D + D_t$ $\quad C_\mu = 0.09$ $\quad Sc_t = 0.7$

$D_t = \mu_t/\rho Sc_t$

Special attention in the numerical studies of this subject is paid to motion modeling. They can be divided into two general types: indirect and direct. Indirect methods, such as the momentum source and turbulent kinetic energy source, have been used in a limited number of studies owing to their low computational cost. Because the mesh recovery process is not required in the indirect methods, these methods are faster than the direct methods; however, the results are widely dependent on the source term and cannot be uniquely measured. By contrast, the direct method is preferred in such studies, and the mesh update method is used to renew the surrounding moving mesh. Although both direct and indirect methods have advantages and disadvantages, direct methods to study the characteristics of the current created by the moving movement can be more reliable, and the use of direct methods by renewing the mesh with current computer equipment is possible. Dynamic or moving mesh methods divide the computational domain into static and dynamic mesh regions. The layering grid updating of the dynamic mesh method changes the deformed grids owing to the motion. Springing-based smoothing and local re-meshing methods are used to model the boundary motion. In the smoothing method, initially, the grid lines form a hypothetical spring set with an initial balance, which causes movement in the spring set and creates a new balance by creating a force. The spring-based smoothing method only adjusts cell node positions instead of cell numbers; thus, solution divergence owing to negative cell volume is inevitable in large boundary displacements. The local re-meshing method updates the cell numbers according to skewness

ACCEPTED MANUSCRIPT

or size criteria. The dynamic layering method adds or deletes layers of boundary-adjacent cells with the layer's height in comparison with an ideal cell height and split and collapse factors.

In numerical predictions, the velocity, temperature and concentration profiles are usually employed for verification of the results. The comparisons are performed either with own experiments, or basic test cases such as natural convection in a cavity [25], or flow in a ventilated room [26-28].

4. Human Motion

Typically, a moving object in a ventilated room is a human. The presence of humans in clean rooms is inevitable, and ignoring this can reduce the accuracy of the results. On the one hand, the presence of humans changes the flow direction and its velocity magnitude, and on the other hand, it is the pollution main source in such spaces.

There are different tactics to consider human shape and motion. The shape varies from a simple block to a real human. The motion path was divided into walking in a room and passing through the door. Among first publications which consider motion in a ventilated room, Bjorn et al. [29] used two breathing thermal manikins one sitting and one walking on a trolley with a contaminant source on their nose and mouth exhalation. A Binos gas analyzer with N_2O tracer in addition to smoke tests for visualization were employed. The temperature distribution was measured with thermocouples type T. They compared the temperature and contaminant distributions along a vertical line at different motion speeds and concluded that the moving manikin causes air downwards from the upper part of the room into the lower part. Yang and Fu [30] moved a rectangle as an operator in a two-dimensional cleanroom numerically and showed creation of recirculation zones which were remarkably different from those of the moving operator regarded as a stationary object in the cleanroom of the previous studies. Matsumoto and Ohba [31] experimentally assumed a cylinder on an electrical slider to be a

ACCEPTED MANUSCRIPT

moving object in a ventilated room. The measurements of temperature and tracer gas concentration, specifically carbon dioxide, were obtained through the use of C-C thermocouples and a B&K multi-gas monitor, respectively. It is worth noting that the vertical direction of the supply airflow had the most significant influence on air temperature and ventilation effectiveness. Brohus et al. [32] used a simple numerical approach to account for the motion by distributed momentum source and turbulent kinetic energy sources for two kinds of movement in the operating room, namely a significant single-event motion and continuous small-scale local movements. It was found that this motion leads to a local but remarkable bacterial spreading risk. Deng et al. [33] assumed a simple cubic block as a moving body and numerically employed the dynamic mesh technique. They reported that the effect of motion on the velocity field and contaminant concentration with mixing ventilation was greater than that with displacement ventilation. Shih et al. [24] assumed a lying person on a bed and a walking person in an isolated room connecting to an anteroom with a sliding door. They concluded that although the flow field is affected by the moving person but quickly returns to the original state.

Saidi et al. [34] assumed a moving point contaminant source in a cleanroom and reported a great dependency of contaminant dispersion on its source motion and path. They showed an improvement in system performance, namely the final efficiency and spreading radius indexes, when the source motion was in the path of the dominant airflow. In addition, the least source-path dependency was observed in the directional airflow pattern. Wang and Chow [35] studied the effect of human motion on the distribution and deposition of expiratory droplets in an isolation room with same geometry as Shih et al. [24] and found that increased walking speed reduces the total number of suspended droplets; thus, decreasing the infection risk. In another numerical study, Chow and Wang [36] focused on the effect of the surgeon bending movement on the dispersion of bacteria-carrying particles. They concluded that a high bacteria-carrying

ACCEPTED MANUSCRIPT

particle concentration within the surgical critical zones was a result of the increased release rate of bacteria-carrying particles and eddy formation. Han et al. [37] investigated the aerodynamic consequences of human movement in enclosed spaces using a full-scale environment, a life-size thermal manikin, a double-track orbit, and a trolley at moving speeds of 0.5-1.5 m/s. The study revealed that the streamwise velocity profile and wake structure depend on the human profile and moving speed. The findings suggested that human activities such as walking or running can significantly impact the airflow motion in enclosed environments. The aerodynamic effects of human movement are influenced by factors such as moving speed, distance, and spatial location.

Hang et al. [38] found that human motion affects the spread of airborne particles, but ventilation design has a greater impact. They concluded better performance of ceiling-level exhaust than floor-level exhaust with equal air change rate in controlling the transmission of airborne particles. From their numerical results, they observed that a simplified motion of a rectangular block produces a stronger flow disturbance than a realistic human walking. In addition, the importance of human body heating, which produces stronger thermal energy, slightly strengthens airborne transmission. Wu and Gao [39] studied the body motion-induced wake flow and its interaction with human thermal plumes numerically. The heat load of person was assumed 75 W and the range of speed was 0.2-1.0 m/s. Because of the body motion, downwash vortices were produced behind the body's upper part. Considering the buoyancy effects, and at lower speeds, the body thermal plume was comparable with the wake flow. The downwash was substituted by an upward flow in the back of the body at higher motion speeds, i.e. greater than 0.4 m/s. They also reported that after stopping, the recovery time of the airflow was less than that of the contaminant dispersion. Tao et al. [40] conducted a numerical study on human-induced wake flow and particle re-dispersion from floors. Their findings revealed the presence of a recirculation region after the free end of the head, characterized by an upward flow in front

ACCEPTED MANUSCRIPT

of the upper body and a downwash flow at the back, where the highest velocity in the flow field occurs. At the lower part of the body, the wake flow gradually became horizontal due to the suppression of the airflow from the upper body. However, the airflow induced by the lower part of the legs resulted in an upward trend of airflow, which became the primary mechanism for particles to lift off the ground. Behind the moving manikin, a pair of counter-rotating vortices was formed, with one convecting off the head and another from the gap between the legs, and extending downwards in the wake region.

Cao et al. [41] compared the moving mesh and momentum source term in Navier-Stokes equations to simulate a moving object with velocity of 0.1 m/s in a one cubic meter chamber. They performed a series of experiments to validate their simulations employing hotwire and particle counter for velocity and concentration measurements. They showed that the momentum source method, in comparison to the dynamic mesh method, with less than 90% computational cost, leads to 15% and 5% deviation in flow and particle, respectively. Eslami et al. [42] modeled a walking visitor with real geometry in a hospital isolation room with nurses and patients. The room dimensions were $2.9\times3.7\times2.55$ m^3 and the moving speed range was 0.25-1.0 m/s. The recirculation zones that entrained and entrapped airborne bacteria-carrying particles were released from the visitor's body. They found that a distance below 44 cm between the patient and the visitor led to a remarkable infection. In addition, the walking speed effect on the ventilation system effectiveness was negligible.

Tao et al. [43] employed a smoke technique for visualizing moving objects with different size and shape (standing, walking and larger bodies) with one fifth scale and motion speed of 0.95 m/s. A larger body shape generated weaker upwash flow located downstream of the body and near the ground due to smaller aspect ratio compared to a slim body. Luo et al. [44] measured longitudinal and cross-sectional airflow distributions with different motion speeds by particle image velocimetry (PIV) in a small-scale chamber using a cylinder on a trolly as a moving

ACCEPTED MANUSCRIPT

occupant. The chamber length was 1.45 m with cross section of 0.4 m×0.4 m and the moving speed range was 0.1-0.5 m/s. The motion of the contaminants pattern was upward near the floor along the moving path, symmetric downward, and expansive vortices. Their CFD results were following the PIV-captured vortices.

Liu et al. [45] conducted an experimental and numerical study to investigate the impact of a circulating nurse walking on airflow and particle distribution in the operating room. They used multichannel air velocity acquisition in experiments and the Realizable k-ϵ turbulence model for the air phase, the Lagrangian particle tracking model for the particle phase, and the dynamic mesh model in numerical simulation. The study found that as the walking speed of the circulating nurse increased, the disturbance to airflow also increased significantly, and the length of the wake became larger. At a height of 1 m, when the walking speed was 1 m/s, the wake length was 2.51 m, while the wake length at the same height was 1.31 m when the walking speed was 0.5 m/s. The circulating nurse walking had no effect on the airflow above the operating table, but it did affect the airflow above nearby instrument tables. However, a walking speed of 0.25 m/s caused little disturbance to the airflow above nearby instrument tables, but the bacterial carrying particles concentrations were still not minimal. The study was limited by several difficulties in the experiment, such as difficulties in particle release from the walking circulating nurse and in measuring particle concentrations in crucial locations. Therefore, the researchers suggested that future studies should include experimental studies to validate their findings.

Bhattacharya et al. [46] used omnidirectional and ultrasound sensors for indoor air velocity magnitude and components measurements, respectively. They used UC Berkeley's Center for Built Environment chamber with dimensions of 5.48×5.44×2.5 m^3. Investigating the motion of a real human in their study was the first in these studies, and the flow was affected at 1 m distance from the walking line and 10 s time after the passage. They concluded that the

ACCEPTED MANUSCRIPT

similarity between the flow pattern of walking once and twice has the potential to predict the flow patterns of a random walk from a set of base cases.

Furthermore, it was discovered in this study that the flow field generated by high-velocity supply air was capable of confining the effects of movement to a very limited area; in other words, the impact of walking movement on the flow properties was more noticeable in the absence of a dominant air supply. Feng et al. [47] studied temperature stratification stability (TSS) and temperature stratification recovery time (TSRT) based on important parameters of manikin moving velocity (v), manikin moving duration (t), manikin heat generation intensity (P) and air change rate of the chamber (ACH). Results showed factors destruct the mean TSS, ranked from the most to least significant, are v, ACH, P and t, and those for mean TSRT are v, t, P and ACH. Lv et al. [48] focused on human walking pattern effect on contaminant dispersion in a residential kitchen and found a mutual effect of the wake and the thermal plume. They used a tracer gas experiment to validate the accuracy of their method. As one progresses parallel to and in the direction of the counter, the airflow becomes significantly disrupted, leading to altered flow characteristics near the range hood. The most profound impact occurs in parallel to the counter motion, due to the combined influence of the wake and thermal plume. Mahaki et al. [49] compared three geometries of rectangular, cylindrical, and human-shaped manikins as moving bodies in a local exhaust ventilation system experimentally and numerically using N2O tracer gas. They observed much stronger turbulence and contaminant spread in rectangular geometry than that generated by human-shaped manikin. In addition, they showed that the manikin similarity of results including flow vectors and capture efficiency with a cylindrical moving object is higher than the results with a flat rectangular plate.

Attention should be paid to the scenes where many people sit, such as aircraft cabins, buses, and offices. Wu et al. [50] conducted a comprehensive experiment to examine the impact of human movement on the exhaled viral aerosols of a seated thermal breathing manikin. In

ACCEPTED MANUSCRIPT

stagnant situations, the concentration of aerosols diminished swiftly beyond a distance of 1.5 m from the source individual. However, when the moving manikin moved in the same direction as the seated manikin's exhalation, the high-risk range extended from 1.5 m to 3 m forward, and the lateral range increased from 1.3 m to 2 m. In addition, Wu et al. [51] investigated the influence of interactive human movement on the exhalation of seated patients, which poses a greater threat than standing patients. They discovered that the impact of human movement on indoor airflow and droplet dispersion can persist for over two minutes, attributable to turbulence and heightened indoor convection. Consequently, individuals in the affected area may be exposed to an increased risk even after the movement has ceased.

Belut et al. [52] studied a moving obstacle wake flow numerically with LES model and experimentally in a room with various obstacles necessary for their instrumentation. An open cavity was used behind the moving body to emit the tracer gas continually. They found that the contaminant concentration peaks depend on the room's initial turbulent state up to two times which is an important consequence in the field of risk management measures.

The significance of the source of particle release and the initial condition of contaminant distribution is a critical assumption in the study. Tan et al. [53] created a model of an isolation ward with dimensions of 6×4.2×3 m^3 with two floor-level exhaust outlets and four ceiling-mounted air diffusers equipped with HEPA filters. Thus, the model assumed that no particles were injected through the diffuser inlets. The heat flux from the medical staff and patient bodies was 116 W/m^2 and 58 W/m^2, respectively. Pathogenic particles with a diameter of 5 μm and a density of 2 g/cm^3 were released from the medical staff's body at a rate of 1.31×10^{-12} kg/s (600 particles/min). They concluded that higher walking speed of 1 m/s produced a significant secondary airflow of 1.12 m/s, while 0.25 m/s and 0.5 m/s generated lower secondary airflows of 0.41 m/s and 0.53 m/s, respectively. The number of particles settled on the patient at 0.25 m/s, 0.50 m/s, and 1 m/s were 31, 18, and 5, respectively. The findings suggest that a higher

ACCEPTED MANUSCRIPT

walking speed reduces the number of particles settled, according to the assumptions made in the study.

Indoor occupant motion is an inherent disturbance source that can compromise the effectiveness of vertical thermal stratification and the ventilation system in a displacement ventilation environment. While it is well-established that occupant motion can adversely impact these systems, the specific mechanisms by which this occurs are not yet fully understood. To address this knowledge gap, Lu et al. [54] employed a numerical simulation to examine how occupant motion affects vertical thermal stratification. The study showed that the primary cause of the weakening of the vertical thermal stratification is the reverse horizontal flow generated by the collision of the wake with the walls. During this process, the vertical thermal profile undergoes four stages. Initially, the profile shape changes, followed by a uniform translation. Subsequently, temperature variations occur only near the floor, and finally, the indoor temperature stabilizes even as occupants continue to move around. It was found that when human bodies move at normal speeds ranging from 1.0 m/s to 1.6 m/s, the temperature gradient can decrease by approximately 45.0% to 75.7%.

The realism of human motion mechanisms has advanced in recent years. In a study conducted by Jo et al. [55], realistic walking motions, including shoulder, hip, and knee movements, were analyzed numerically in a layout of an airborne infection isolation room. The results showed that the horizontal movement increased the leakage rate to 20.6%, which further increased to 28.6% when realistic walking motions were implemented. Although the study focused on cleanrooms, which have higher ventilation rates than typical spaces, the implications extend beyond these settings. The influence of realistic human movement on airflow and contaminant dispersion in general areas may be even more significant, indicating a potential area for further research.

ACCEPTED MANUSCRIPT

5. Door Motion

The motion of the door disturbs the flow pattern and creates vortices that affect both airflow and particle distribution. There are two main categories of door motion in cleanrooms: sliding and hinged doors. The source of the contaminant position and the two sides of the door pressure difference affects the results including flow field and particle behavior. In some studies, a person passing across the door has also been studied. Shih et al. [24] investigated a sliding door and a moving person in an operating room using a dynamic mesh numerical method. Sudden pressure variation in the isolation room during the door opening and closing periods showed an obvious effect on the internal pressure and velocity distributions. They concluded that contaminant transport is affected only by the magnitude of the specified pressure difference during door opening.

In variety of experimental studies, instead of air, water is chosen because of easier visualization using colored dye. Tang et al. [56] carried out experiments in water, at equivalent Reynolds with the full-scale situation in air. They compared different door types of single and double hinged and sliding doors and found that double-hinged doors lead to the highest leakage and sliding doors cause the greatest contamination in moving human cases. Their experiments showed a better performance of the sliding doors compared to the hinged doors. Fontana and Quintino [57] also used water tank and designed a differential pressurization system to study the effect of hinged doors on the contamination transfer between dirty and clean rooms with and without pressure difference in two sides of the door. They concluded that the dirty air volume transferred to the cleanroom is independent of the differential pressures and flow rate imbalance but is related to the displaced volume during door opening. Hathway et al. [58] studied air exchange and infection spread due to hinged doors motion using concentration measurements of Rhodamine WT in a water tank medium. The determination of Rhodamine concentrations was accomplished employing a Cyclops fluorometer Turner Designs, which

ACCEPTED MANUSCRIPT

was linked with an analog-to-digital converter, and the data acquisition was performed utilizing TracerDAQ® software. They found a linear relationship between door hold-open time and the volume flux between rooms. They observed that opening and closing stages form and move a large-scale jet-like vortex. The effect of hold-open time on volume flux between rooms showed a range of 67% to 98% of the volume swept by the door for a full scale hold open time between 6.67 s and 26.67 s.

Kalliomaki et al. [59] used a real scale room employing B&K multi-gas analyzer with Sulphur hexafluoride (SF6) and Nitrous Oxide (N2O) as tracer gases to determine the transferred volume in both directions across the doorway. In addition, they used a smoke machine (Martin Magnum 550) to visualize the airflow with its almost neutrally buoyant particle size of around 1-1.5 μm suitable for pattern visualization. They compared hinged doors and sliding doors and found higher exchange between rooms in hinged door. Also, the dependency of exchange on human passage and direction was greater in the hinged doors than in sliding doors. Hendiger et al. [60] focused on the effect of pressure differences and hinged door swing direction on contaminant motion between adjacent rooms in the range of 2.5-50 Pa. Positioning a fog generator as a heavy contaminant in a negative room and visualizing the contaminant distribution showed that the door swinging towards negative pressure contaminated room and its slower opening reduced the contaminant transfer.

Kalliomaki et al. [61] studied different scenarios experimentally with smoke visualization in two real scale adjacent rooms and found lower airflow generation across doorways in sliding doors than hinged doors. Tracer gas measurement showed that the exchanged air volume of hinged door was 2-3 times than the sliding door in air changes per hour of 6 and 12 and with and without passage scenarios. They suggested sliding doors as prime door types in the isolation rooms. Lee et al. [62] showed increased interzonal air volume exchange over the doorway with increased temperature difference. They found an obvious decrease of interzonal

ACCEPTED MANUSCRIPT

air exchange volume through the doorway in sliding door than hinged door, for isothermal conditions. However, the interzonal air exchange volume through the doorway were not significantly different in two door types when a temperature difference between areas was involved.

Mousavi et al. [63] compared numerical results from 2D and 3D assumptions and less than 8% difference in air exchange volume was observed. They released 500 particles of 1 μm diameter at an anteroom-isolation room doorway. Discrete phase of particles was solved by assuming drag, Saffman lift, virtual mass, and pressure gradient forces. In addition, the Cunningham correction coefficient (1.1614) was applied to modify the slip effect on the small particle size and the discrete random walk model was applied to capture the stochastic behavior of particles. Higher hinged door speeds created turbulence and increased the exchange volume rate in neutral and negative pressure situations.

Villafruela et al. [64] studied three experimental tests series of a) door opening-closing, b) door opening, a person entering the operating room and the door closing, and c) door opening and a person leaving the operating room and door closing. They found that passage direction has a significant influence on the exchange volume across sliding doors in an operating room. Also, the air volume entering the operating room was higher on the closer side of the person to the doorframe, and moving away from the doorframe reduced the inward air. Leaving persons cause air entering to the operating room, but to a lesser extent than entering.

Chang et al. [20] used an experimental method based on the tracer gas and a full-scale test facility with inner-outer rooms to ensures that the inleakage is purely from the outer room and induced by the person entering. They divided total inleakage into the door pumping volume and person additional volume While, the pumping volume was roughly constant, the swing time did pose a significant effect on the person additional volume. In a numerical study, Chang et al. [23] also found that inleakage occurred throughout the door rotating process. The

ACCEPTED MANUSCRIPT

inleakage flow rate peaked at the beginning and end of the rotating time period, while the flow rate was generally low during the direction-changing period. Chang et al. [21] divided the leakage process for an entering person across a hinged door into four steps: the door draws in air, the person drags air, the closing door cuts off the wake, and the door pushes the air in the last movement. They concluded that the first two stages caused the greatest leakage.

Although airflow leakage can be quantitatively measured using tracer gas techniques, it is challenging to observe the turbulent flow features in detail. Saarinen et al. [19] employed large eddy simulation (LES) in conjunction with experimental measurements and found that, without passage, the air volume leakage across the doorway was initially dominated by vortex shedding in the wake of the door. However, during extended hold-open periods, a possible temperature difference became the predominant driving force. Upon passage, a short and powerful pulse of the leakage flow rate is generated, even if the walker stops to wait for the door to open. Papakonstantis et al. [65] examined the flow transfer in a hinged door using colored water entering the second room by a rotating cloud, initially almost axisymmetric, and then three-dimensional in the opening door stage. A great vortex was generated owing to the door closing, which propagated along the vertical walls and grew and occupied most of the space. They reported velocity vectors near the door experimentally using TSI volumetric 3-component velocimetry (V3V) system based on the defocusing technique and three independent cameras. Sadrizadeh et al. [66] indicated a significant change in operating room positive pressure during door opening periods. They conducted an investigation into the functionality of sliding and hinged doors in an operating room that was subjected to an over-pressurization of approximately 15 Pa, in comparison to the adjacent corridors. The study aimed to assess the effectiveness of positive-pressure systems in preventing the infiltration of bacteria-carrying particles from the corridors. However, it was found that frequent door openings could interfere with airflow ventilation systems, alter the pressure gradient, and increase the risk of infection

ACCEPTED MANUSCRIPT

for patients undergoing surgical procedures. This disturbance in the airflow field could potentially result in containment failure. This leads to a failure in isolation conditions and disperses the infectious flow, and the ventilation system will not produce the required positive pressure, which causes the infectious particles dispersion. They believed that frequent door openings threaten the positive pressure and are a risk for operating rooms. Various parameters such as cooling load, temperature, relative humidity, air cleanliness level, and air exchange rate play a crucial role in determining the temperature difference between cleanrooms and adjacent rooms. This difference creates an air convection between the two spaces, which is a critical factor in maintaining optimal conditions for air quality and energy consumption.

Zhou et al. [67] modeled a sliding door in a hospital operating room and found that a higher operating room temperature than the anteroom helped protect the clean environment. Lind et al. [68] used low-velocity wall diffuser ventilation to minimize the airborne particle movement to the operating room in door opening periods. The study's numerical outcomes indicated that a system employing high airflow rates diffusely from the anteroom to the corridor during door openings can effectively decrease the amount of potentially contaminated air from the corridor into the anteroom.

Shao et al. [14] used a particle counter measurement device and found that personnel passage through the door leads to the sudden rise of the particle concentration near the doorway of the clean area. A highly contaminated environment in the airlock was considered to evaluate the impact of human movement passing a door on short-term contamination in the cleanroom. The initial steady concentration of 0.5 and 1 μm particles in the cleanroom was within the range of Classes 6 to 7, as defined by ISO 14644-1, with counts ranging from 18,519 to 100,482 in m^3. When personnel passed at a doorway flow rate of 210 L/s (air speed of 0.11 m/s), the overall cleanroom environment was degraded to ISO Class 8 within a short period of time, while the zonal environment near the doorway became more contaminated. However, when the airflow

ACCEPTED MANUSCRIPT

through the doorway was increased to approximately twice the initial rate (air speed of 0.22 m/s), the containment effectiveness was greatly improved, allowing the cleanliness of the overall cleanroom environment to meet Class 7. Additionally, increasing the airflow rate to approximately three times the initial rate (air speed of 0.33 m/s) further improved the containment effectiveness and better controlled the adverse effects of personnel movement on the cleanroom environment.

Wang et al. [69] modeled a sliding door in a hospital operating room and considered two thermal conditions of summer and winter with higher and lower temperatures in the operating room than in the corridor, respectively. In their examined case, a three Celsius temperature difference as a driving force caused 2.1 CFU/m^3 contamination, which showed the importance of controlling the temperature of the operating room and adjacent spaces. In addition, studying different exhaust flows showed that a 20-30% decrease in the exhaust could reduce the airborne contaminant to a sufficiently small level.

Alonso et al. [70] employed ultrasound anemometry and found that the greatest air entry from adjacent areas occurred when the door was opened; thus, it might suggest keeping the doors open during surgeries instead of frequently entering and leaving. Moreover, hinged doors cause a change in airflow during the process of opening and closing, which adversely affects the flow pattern and results in an increased amount of air entering the operating room. Wu et al. [71] modeled the hinged door and compared the air exchange in different rotation speeds and temperature differences. The temperature difference indoors and outdoors below two Celsius showed negligible effects while above three Celsius could significantly affect the airflow pattern. Reduced air exchange because of thermal effects was observed in the door-opening directions toward the room at higher temperatures.

Shao et al. [72] used smoke in a mesh-wall room and observed the smoke invasion through a hinged door. The initial pressure difference, airlock situation, and the airlock doors' delay time

ACCEPTED MANUSCRIPT

were studied, and it was found that the combination of delay time and differential pressure improves the performance. A cycle time of 4.5 s and a pressure difference of 5-25 Pa between two rooms showed that a pressure difference of 5 and 10 Pa was inadequate to suppress smoke invasion under the studied conditions. Installing an airlock between the cleanroom and the polluted space had a buffer effect with a less than 5 Pa pressure difference. Zheng et al. [73] studied the effects of hinged doors and human motion and found complex unsteady flows that transport noteworthy aerosols among pressure-equilibrated rooms. They suggested that the slow opening and fast closing of the inward-facing door into an aerosol-rich room decreases aerosol transport.

Conclusions

Motion effects including human and door on the flow and airborne particles have been reviewed. Controlling indoor areas has different applications and the recent prevalence of infectious diseases such as COVID-19 adds to the importance of the subject.

This review reveals the obvious effects of motion in cleanrooms, as summarized in Table 2, where the control of airborne particle distribution is of high priority. Mentioned studies approved that human motion and door opening and closing are substantial transport mechanisms that must be considered in measuring airborne disease transmission hazards and authorizing strategies to decrease contaminant transmission. There are several suggestions for further research. The verification of numerical models with reliable experimental measurements could be helpful. Considering real heat loads, real human motion, parametric studies of different supply and exhaust flow rates, contaminant source locations, and traffic patterns are among the subjects open to work. According to approximately fifty published studies, several key findings have emerged. These include a reduction in the cleanroom classification, a decrease in temperature gradient by one third and one fourth, an increase in

ACCEPTED MANUSCRIPT

contaminants and secondary flow depth by two or three times, and particle settlement on the patient multiplying six times. Additionally, there is a need for redesigning the ventilation system. Further research is necessary to fully understand the implications of these findings, particularly in terms of their application. Moreover, both experimental and numerical studies must consider the importance of motion to achieve accurate results. Further research is necessary to enhance the quantitative results of experiments, while an increased number of them are qualitative results.

Conflict of interest

The authors declare that they have no conflict of interest.

Acknowledgement

This research was performed during industrial sabbatical of first author in summer 2023 in Savis Sanat Asia cleanroom engineering department. Authors would like to thank Savis Sanat Asia company and Razi university.

Table 2. Overview of published works studying the motion effect on flow and particle distribution

Authors	Motion type	Application	Technique	Description and finding
Bjorn et al., 1997	Human	Ventilated room	Experiment	Sitting and walking manikin and experimental situations had a significant effect on contaminant distributions.
Yang and Fu, 2002	Human	cleanroom	CFD	Recirculation zones were observed in a two-dimensional numerical study.
Matsumoto and Ohba, 2004	Human	Ventilated room	Experiment	Moving style and velocity had a noteworthy effect on the distribution of the temperature and effectiveness of the ventilation system.
Brohus et al., 2006	Human	Operating room	CFD	The motion caused a local but serious transport risk of bacteria from the non-clean to the clean region.
Deng et al., 2007	Human	Ventilated room	CFD	Motion effect on velocity field and contaminant concentration with mixing ventilation is greater than with displacement ventilation.
Shih et al., 2007	Human and sliding door	Hospital isolating room	CFD	Contaminants' removal from the source was independent of moving speed. Contaminant transport was affected by the specified pressure difference magnitude during the door opening.
Saidi et al., 2011	Point contaminant source	cleanroom	CFD	Contaminant source movement and path had a great impact on the contaminant distribution.
Wang and Chow, 2011	Human	Hospital isolating room	CFD	Human walking disturbed the local velocity field with wake formation. Increased walking speed reduced the overall number of suspended droplets.

ACCEPTED MANUSCRIPT

Chow and Wang, 2012	Human	Operating room	CFD	Periodic surgeon bending motion affects the airflow and particle distribution.
Tang et al., 2013	Single/double hinged/sliding doors and human	Hospital isolating room	Experiment: food dye in water	Double-hinged doors had the greatest leakage. Sliding doors had the greatest contamination in moving human cases. In total, the sliding doors showed better performance for hospital isolation rooms.
Fontana & Quintino, 2014	Hinged door	Adjacent dirt and clean rooms	Experiment: ink in water	Independence of dirty air volume transferred to the cleanroom on the pressure difference and the flow rate imbalance but related to the displaced air volume in the door opening period.
Han et al., 2014	Human	Still cabin	CFD and experiment	The aerodynamic effects of human movement are influenced by factors such as moving speed, distance, and spatial location.
Hang et al., 2014	Human	Hospital isolating room	CFD	The importance of thermal plumes, ventilation design, and realistic motion was reported.
Wu & Gao, 2014	Human	Ventilated room	CFD	Contaminant dispersion depended on the motion speed and the thermal plume could be ignored in wake dynamics near a moving body at higher speeds.
Hathway et al., 2015	Hinged door	Office and hospital	Experiment: colored food dye in water	Door motion led to a large-scale jet-like flow motion.
Kalliomaki et al., 2015	Hinged/sliding doors	Hospital isolation room	Experiment: smoke	Sliding door induced smaller volume exchange than a hinged door.
Tao et al., 2016	Human	Still room	Experiment: smoke	Behind the moving manikin, a pair of counter-rotating vortices was formed.
Chang et al., 2016a	Sliding door	Control room	CFD	The inleakage flow rate peaked at the beginning and end of the rotating time period, while the flow rate was generally low during the direction-changing period.
Chang et al., 2016b	Sliding door	Control room	Experiment	The pumping volume was roughly constant, the swing time did pose a significant effect on the person additional volume.
Hendiger et al., 2016	Hinged door	Heavy contaminant	Experiment: dense smoke	The door swinging towards negative pressure and its slower opening reduced the contaminants transfer.
Kalliomaki et al., 2016	Hinged/sliding doors	Hospital isolation room	Experiment: smoke	In different realistic operation scenarios, the single sliding door showed better performance than the single hinged door.
Lee et al., 2016	Hinged/sliding doors	Office building	CFD and experiment	The interzonal air volume exchange across the doorway was increased with increasing temperature differences. It was much more impressive for the sliding door.
Mousavi et al., 2016	Hinged door	Hospital isolation room	CFD	Comparing results from 2D and 3D assumptions showed less than 8% difference in air exchange volume. Higher door speeds created turbulence and increased the rate of volume exchange under both neutral and negative pressure situations.
Villafruela et al., 2016	Sliding door and human	Operating room	Experiment: smoke	The air volume entering the operating room was higher on the closer side of the person to the doorframe.
Cao et al., 2017	Human	A chamber with a particle source at the inlet	CFD	Human motion affected surrounding airflows and dispersion of particle concentration. Faster walking led to longer particles decay.
Chang et al., 2017	Hinged door and human	Control room	CFD: SF6 as tracer	The leakage process for an entering person across a hinged door into four steps was divided to: the door draws in air, the person drags air, the closing door cuts off the wake, and the door pushes the air in the last movement. They concluded that the first two stages caused the greatest leakage.
Eslami et al., 2017	Human	Hospital	CFD	Importance of distance between the patient and visitor on infection level and negligible effect of motion velocity on the ventilation effectiveness index.
Saarinen et al., 2018	Sliding door and human	Isolation room	Experiment and CFD	During extended hold-open periods, a possible temperature difference became the predominant driving force.
Tao et al., 2018	Human	Still room	Experiment: smoke	Visualizing moving objects with different size and shapes of standing, walking and larger bodies.
Luo et al., 2018	Human	Test chamber	Experiment and CFD: PIV	Released contaminants from the human body would converge and then quickly reach the floor then disperse to the surrounding region.
Papakonstantis et al., 2018	Hinged door	Two equal-size rooms	Experiment: colored food dye in water	The colored water entered the second room by a rotating cloud, initially almost axisymmetric, then became three-dimensional in the opening door stage. A large vortex was generated with the door closing which propagated along the vertical walls, grew, and occupied most of the domain.

ACCEPTED MANUSCRIPT

Sadrizadeh et al., 2018	Hinged/sliding doors	Hospital isolation room	CFD	Frequent door openings threaten the positive pressure and potentially jeopardize the operating rooms
Zhou et al., 2018	Sliding door	Operating room	CFD	The higher temperature of the operating room than the anteroom helped to protect the clean environment.
Lind et al., 2019	Sliding door and human	Operating room	CFD	High air volume into the operating room over low-velocity wall diffusers ventilation unit reduced the entrance of contaminants to the operating rooms during door-opening periods.
Liu et al., 2020	Human	Operating room	CFD and experiment	As the walking speed of the circulating nurse increased, the disturbance to airflow also increased significantly, and the length of the wake became larger.
Shao et a., 2020	Hinged door and human	Pharmaceutical cleanroom	Experiment: particle counter	The personnel passage across the doorway led to a sudden rise of particles near the doorway area of the cleanrooms.
Bhattacharya et al., 2021b	Human	Chamber	Experiment	The walking effect on the airflow was not negligible and created a noteworthy change in the air velocity normal to the walking direction.
Wang et al., 2021	Sliding door	Operating room	CFD	Exhaust flow reduction of the operating room decreased the airborne contamination to a satisfactorily low value.
Feng et al., 2021	Human	Displacement ventilated room	Experiment	Temperature stratification versus manikin moving velocity (v), manikin moving duration (t), manikin heat generation intensity (P) and air change rate of the chamber (ACH).
Alonso et al., 2022	Sliding door	Operating room	Experiment: ultrasound anemometry	The greatest air entry from adjacent areas occurred in the opening door period; thus, it might suggest keeping the doors open during surgery instead of frequently entering and leaving.
Lv et al., 2022	Human	Kitchen	Experiment and CFD	The mutual effect of the wake flow and thermal plume caused the dispersion of contaminants.
Mahaki et al., 2022	Human	Control room	Experiment and CFD	Similarity of results of manikin geometry with a cylindrical moving object is higher than the results with a flat rectangular plate.
Wu et al., 2022a	Human	Ventilated room	Experiment	Examining the impact of human movement on the exhaled viral aerosols of a seated thermal breathing manikin.
Wu et al., 2022b	Hinged door	Thermally stratified room	CFD	In thermally stratified environments, considering buoyancy force and door swing, a moderate door velocity led to a minimum air exchange.
Wu et al., 2023	Human	Ventilated room	CFD	influence of interactive human movement on the exhalation of seated patients, which poses a greater threat than standing patients.
Belut et al., 2023	Human	Laboratory	Experiment and CFD: PIV	The transient wake of a moving obstacle was studied and variation of contaminant concentration peaks were observed in different initial room turbulent states.
Shao et al., 2023	Hinged door and human	Pharmaceutical cleanroom	Experiment: smoke	The initial pressure difference, airlock situation, and the airlock doors' delay time were studied, and it was found that the combination of delay time and differential pressure improves the performance.
Zheng et al., 2023	Hinged door and human	Operating room	CFD	Slow opening and fast closing of inward-facing doors in aerosol-rich rooms decrease aerosol transport.
Tan et al., 2023	Human	Isolation room	CFD	Higher walking speed reduces the number of particles settled, according to the assumptions made in the study.
Lu et al., 2024	Human	Displacement ventilated room	CFD	When human bodies move at normal speeds ranging from 1.0 m/s to 1.6 m/s, the temperature gradient can decrease by approximately 45.0% to 75.7%.
Jo et al., 2024	Human	Isolation room	CFD	The horizontal movement increased the leakage rate to 20.6%, which further increased to 28.6% when realistic walking motions were implemented.

ACCEPTED MANUSCRIPT

References

[1] N.P. Cheremisinoff, Handbook of air pollution prevention and control, Elsevier (2002).

[2] B. Brunekreef, B. Forsberg, Epidemiological evidence of effects of coarse airborne particles on health, European respiratory journal, 26(2) (2005) 309-318.

[3] C.A. Pope, D.W. Dockery, Health effects of fine particulate air pollution: lines that connect, Journal of the air & waste management association, 56(6) (2006) 709-742.

[4] S.D. Adar, P.A. Filigrana, N. Clements, J.L. Peel, Ambient coarse particulate matter and human health: a systematic review and meta-analysis, Current environmental health reports, 1 (2014) 258-274.

[5] C. Liu, J. Cai, R. Chen, F. Sera, Y. Guo, S. Tong, ... & H. Kan, Coarse particulate air pollution and daily mortality: a global study in 205 cities, American journal of respiratory and critical care medicine, 206(8) (2022) 999-1007.

[6] P. Naughton, History of cleanrooms, ASHRAE Journal, 61(11) (2019) 38-54.

[7] W. Whyte, Cleanroom technology: fundamentals of design, testing and operation, John Wiley & Sons (2010).

[8] J.W. Useller, Clean room technology, Technology Utilization Division, National Aeronautics and Space Administration, (1969).

[9] W.J. Whitfield, State of the art (contamination control) and laminar air-flow concept, Conference on Clean Room Specifications, Sandia Corporation, (1963) 73-84.

[10] Z. Liu, M. Wu, H. Cao, Y. Wang, R. Rong, H. Zhu, Influence of the visitor walking on airflow and the bioaerosol particles in typical open tomb chambers: An experimental and case study, Buildings, 11(11) (2021) 538.

[11] E.S. Mousavi, R. Jafarifiroozabadi, S. Bayramzadeh, A. Joseph, D. San, An observational study of door motion in operating rooms, Building and environment, 144 (2018) 502-507.

[12] A. Bhattacharya, A.R. Metcalf, A.M. Nafchi, E.S. Mousavi, Particle dispersion in a cleanroom -effects of pressurization, door opening and traffic flow, Building Research & Information, 49(3) (2021a) 294-307.

[13] S. Sadrizadeh, A. Aganovic, A. Bogdan, C. Wang, A. Afshari, A. Hartmann, ... & G. Cao, A systematic review of operating room ventilation, Journal of Building Engineering, 40 (2021) 102693.

[14] X. Shao, K. Hashimoto, L. Fang, A.K. Melikov, K.G. Naydenov, C. Rasmuseen, Experimental study of airborne particle transmission through the doorway of a cleanroom due to the movement of a person, Building and environment, 183 (2020) 107205.

[15] S.B. Poussou, S. Mazumdar, M.W. Plesniak, P.E. Sojka, Q. Chen, Flow and contaminant transport in an airliner cabin induced by a moving body: Model experiments and CFD predictions, Atmospheric Environment, 44(24) (2010) 2830-2839.

[16] H. Zhou, K. Zhong, H. Jia, Y. Kang, Analysis of the effects of dynamic mesh update method on simulating indoor airflow induced by moving objects, Building and Environment, 212 (2022) 108782.

[17] A. Kokkonen, M. Hyttinen, R. Holopainen, K. Salmi, P. Pasanen, Performance testing of engineering controls of airborne infection isolation rooms by tracer gas techniques, Indoor and Built Environment, 23(7) (2014) 994-1001.

[18] P.E. Saarinen, P. Kalliomäki, J.W. Tang, H. Koskela, Large eddy simulation of air escape through a hospital isolation room single hinged doorway -validation by using tracer gases and simulated smoke videos, PloS one, 10(7) (2015) e0130667.

[19] P. Saarinen, P. Kalliomäki, H. Koskela, J.W. Tang, Large-eddy simulation of the containment failure in isolation rooms with a sliding door -An experimental and modelling study, Building simulation, 11, (2018) 585-596.

[20] L. Chang, X. Zhang, Y. Cai, Experimental determination of air inleakage to pressurized main control room caused by personnel entering, Building and Environment, 99 (2016b) 142-148.

[21] L. Chang, S. Tu, W. Ye, X. Zhang, Dynamic simulation of contaminant inleakage produced by human walking into control room, International Journal of Heat and Mass Transfer, 113 (2017) 1179-1188.

ACCEPTED MANUSCRIPT

[22] W. Gao, X. Xie, Y. Liu, X. Chen, C. Zhu, Numerical simulation of the transport of breath-exhaled aerosol from manikin with realistic nasal airway over short social distances, Powder Technology, 437 (2024) 119543.

[23] L. Chang, X. Zhang, S. Wang, J. Gao, Control room contaminant inleakage produced by door opening and closing: dynamic simulation and experiments, Building and environment, 98 (2016a) 11-20.

[24] Y.C., Shih, C.C., Chiu, O. Wang, Dynamic airflow simulation within an isolation room, Building and environment, 42(9) (2007) 3194-3209.

[25] P.L. Betts, I.H. Bokhari, Experiments on turbulent natural convection in an enclosed tall cavity, International Journal of Heat and Fluid Flow, 21(6) (2000) 675-683.

[26] X. Yuan, Q. Chen, L.R. Glicksman, Measurements and computations of room airflow with displacement ventilation, ASHRAE Trans., 105 (1999) 340-352.

[27] F. Chen, C.M. Simon, A.C. Lai, Modeling particle distribution and deposition in indoor environments with a new drift -flux model, Atmospheric Environment, 40(2) (2006) 357-367.

[28] S.B. Poussou, Experimental investigation of airborne contaminant transport by a human wake moving in a ventilated aircraft cabin, Doctoral dissertation, Purdue University, (2008).

[29] E. Bjorn, M. Mattsson, M. Sandberg, P.V. Nielsen, Displacement ventilation: effects of movement and exhalation, Dept. of Building Technology and Structural Engineering, Indoor Environmental Technology, 70 (1997).

[30] S.J. Yang, W.S. Fu, A numerical investigation of effects of a moving operator on airflow patterns in a cleanroom, Building and environment, 37(7) (2002) 705-712.

[31] H., Matsumoto, Y. Ohba, The influence of a moving object on air distribution in displacement ventilated rooms, Journal of Asian Architecture and Building Engineering, 3(1) (2004) 71-75.

[32] H. Brohus, K.D. Balling, D. Jeppesen, Influence of movements on contaminant transport in an operating room, Indoor air, 16(5) (2006) 356-372.

[33] T. Deng, Q. Zhang, G. Zhang, The influences of moving human in a ventilation room, Proceedings: Building Simulation, (2007) 779-786.

[34] M. H. Saidi, B. Sajadi, G.R. Molaeimanesh, The effect of source motion on contaminant distribution in the cleanrooms, Energy and Buildings, 43(4) (2011) 966-970.

[35] J. Wang, T.T. Chow, Numerical investigation of influence of human walking on dispersion and deposition of expiratory droplets in airborne infection isolation room, Building and Environment, 46(10) (2011) 1993-2002.

[36] T.T. Chow, J. Wang, Dynamic simulation on impact of surgeon bending movement on bacteria-carrying particles distribution in operating theatre, Building and environment, 57 (2012) 68-80.

[37] Z. Han, W. Weng, Q. Huang, Numerical and experimental investigation on the dynamic airflow of human movement in a full-scale cabin, HVAC&R Research, 20(4) (2014) 444-457.

[38] J. Hang, Y. Li, R. Jin, The influence of human walking on the flow and airborne transmission in a six-bed isolation room: Tracer gas simulation, Building and Environment, 77 (2014) 119-134.

[39] Y. Wu, N. Gao, The dynamics of the body motion induced wake flow and its effects on the contaminant dispersion, Building and environment, 82 (2014) 63-74.

[40] Y. Tao, K. Inthavong, J. Tu, Computational fluid dynamics study of human-induced wake and particle dispersion in indoor environment, Indoor and Built Environment, 26(2) (2017) 185-198.

[41] S.J. Cao, D. Cen, W. Zhang, Z. Feng, Study on the impacts of human walking on indoor particles dispersion using momentum theory method, Building and Environment, 126 (2017) 195-206.

[42] J., Eslami, A. Abbassi, M.H. Saidi, Numerical simulation of the effect of visitor's movement on bacteria-carrying particles distribution in hospital isolation room. Scientia Iranica, 24(3) (2017) 1160-1170.

[43] Y. Tao, K. Inthavong, P. Petersen, K. Mohanarangam, W. Yang, J. Tu, Experimental visualisation of wake flows induced by different shaped moving manikins, Building and Environment, 142 (2018) 361-370.

ACCEPTED MANUSCRIPT

[44] N. Luo, W. Weng, X. Xu, M. Fu, Human-walking-induced wake flow–PIV experiments and CFD simulations, Indoor and Built Environment, 27(8) (2018) 1069-1084.

[45] Z. Liu, H. Liu, R. Rong, G. Cao, Effect of a circulating nurse walking on airflow and bacteria-carrying particles in the operating room: An experimental and numerical study, Building and Environment, 186 (2020) 107315.

[46] A. Bhattacharya, J. Pantelic, A. Ghahramani, E.S. Mousavi, Three-dimensional analysis of the effect of human movement on indoor airflow patterns, Indoor Air, 31(2) (2021b) 587-601.

[47] L. Feng, F. Zeng, R. Li, R. Ju, N. Gao, Influence of manikin movement on temperature stratification in a displacement ventilated room, Energy and Buildings, 234 (2021) 110700.

[48] L. Lv, Y. Wu, C. Cao, L. Zeng, J. Gao, W. Xie, J. Zhang, Impact of different human walking patterns on flow and contaminant dispersion in residential kitchens: Dynamic simulation study, Building Simulation, Tsinghua University Press, (2022) 1-16.

[49] M. Mahaki, M. Mattsson, M. Salmanzadeh, A. Hayati, Experimental and numerical simulations of human movement effect on the capture efficiency of a local exhaust ventilation system, Journal of Building Engineering, 52 (2022) 104444.

[50] J. Wu, W. Weng, M. Fu, Y. Li, M. Lan, Enhancement effect of human movement on the high risk range of viral aerosols exhaled by a sitting person, Building and Environment, 218 (2022a) 109136.

[51] J. Wu, W. Weng, M. Fu, Y. Li, Numerical study of transient indoor airflow and virus-laden droplet dispersion: Impact of interactive human movement, Science of The Total Environment, 869 (2023) 161750.

[52] E. Belut, S. Lechene, B. Trouette, S. Vincent, G.H. Atallah, Flow and contaminant transfer at the interface of an aerodynamic containment barrier subjected to the wake of a moving obstacle. Building and Environment, 241 (2023) 110465.

[53] H. Tan, K.Y. Wong, M.H.D. Othman, B.B. Nyakuma, D.D.C.V. Sheng, H.Y. Kek, ... & I.H. Hatif, Does human movement-induced airflow elevate infection risk in burn patient's isolation ward? A validated dynamics numerical simulation approach, Energy and Buildings, 283 (2023) 112810.

[54] F. Lu, X. Lingjun, C. Min, W. Yan, G. Naiping, Dynamic effects of occupant motion on indoor vertical thermal stratification in the displacement ventilation system, Energy and Buildings, 304 (2024) 113843.

[55] S. Jo, G. Kim, M. Sung, A study on contaminant leakage from Airborne Infection Isolation room during medical staff entry; Implementation of walking motion on hypothetical human model in CFD simulation, Journal of Building Engineering, 86 (2024). 108812.

[56] J. W. Tang, A. Nicolle, J. Pantelic, C.A. Klettner, R. Su, P. Kalliomaki, ... & K.W. Tham, Different types of door-opening motions as contributing factors to containment failures in hospital isolation rooms, PloS one, 8(6) (2013) e66663.

[57] L. Fontana, A. Quintino, Experimental analysis of the transport of airborne contaminants between adjacent rooms at different pressure due to the door opening. Building and environment, 81 (2014) 81-91.

[58] A. Hathway, I. Papakonstantis, A. Bruce-Konuah, W. Brevis, Experimental and modelling investigations of air exchange and infection transfer due to hinged-door motion in office and hospital settings, International Journal of Ventilation, 14(2) (2015) 127-140.

[59] P. Kalliomäki, P. Saarinen, J.W. Tang, H. Koskela, Airflow patterns through single hinged and sliding doors in hospital isolation rooms, International Journal of Ventilation, 14(2) (2015) 111-126.

[60] J. Hendiger, M. Chludzinska, P. Zietek, Influence of the pressure difference and door swing on heavy contaminants migration between rooms, PloS one, 11(5) (2016) e0155159.

[61] P. Kalliomaki, P. Saarinen, J.W. Tang, H. Koskela, Airflow patterns through single hinged and sliding doors in hospital isolation rooms -Effect of ventilation, flow differential and passage, Building and Environment, 107 (2016) 154-168.

[62] S. Lee, B. Park, T. Kurabuchi, Numerical evaluation of influence of door opening on interzonal air exchange. Building and environment, 102 (2016) 230-242.

ACCEPTED MANUSCRIPT

[63] E.S. Mousavi, K.R. Grosskopf, Airflow patterns due to door motion and pressurization in hospital isolation rooms, Science and Technology for the Built Environment, 22(4) (2016) 379-384.

[64] J.M. Villafruela, J.F. San Jose, F. Castro, A. Zarzuelo, Airflow patterns through a sliding door during opening and foot traffic in operating rooms, Building and Environment, 109 (2016) 190-198.

[65] I.G. Papakonstantis, E.A. Hathway, W. Brevis, An experimental study of the flow induced by the motion of a hinged door separating two rooms, Building and Environment, 131 (2018) 220-230.

[66] S. Sadrizadeh, J. Pantelic, M. Sherman, J. Clark, O. Abouali, Airborne particle dispersion to an operating room environment during sliding and hinged door opening, Journal of infection and public health, 11(5) (2018) 631-635.

[67] B. Zhou, L. Ding, F. Li, K. Xue, P.V. Nielsen, Y. Xu, Influence of opening and closing process of sliding door on interface airflow characteristic in operating room, Building and environment, 144 (2018) 459-473.

[68] M.C. Lind, S. Sadrizadeh, B. Venas, P. Sadeghian, C. Wang, T.T. Harsem, Minimizing the airborne particle migration to the operating room during door opening, IOP Conference Series: Materials Science and Engineering, 609 (3) (2019) 032055.

[69] C. Wang, S. Holmberg, S. Sadrizadeh, Impact of door opening on the risk of surgical site infections in an operating room with mixing ventilation, Indoor and Built Environment, 30(2) (2021) 166-179.

[70] J.S.J. Alonso, M.A. Sanz-Tejedor, Y. Arroyo, M.R. San Jose-Gallego, Analysis and assessment of factors affecting air inflow from areas adjacent to operating rooms due to door opening and closing, Journal of Building Engineering, 49 (2022) 104109.

[71] Y. Wu, L. Feng, M. Liu, Z. Wu, N. Gao, Numerical study on transient airflows and air exchange induced by door motion in thermally stratified environment, Building and Environment, 223 (2022b) 109498.

[72] X. Shao, Y. Liu, Y. Hao, X. Wen, C. Li, X. Ma, ... & X. Li, Smoke visualization for the invasion of pollutants during door-opening process in pharmaceutical cleanrooms: Effects of initial pressure differential and airlock barriers, Energy and Buildings, 279 (2023) 112711.

[73] M. Zheng, Y. Fan, X. Li, D. Lester, X. Chen, Y. Li, I. Cole, Aerosol exchange between pressure-equilibrium rooms induced by door motion and human movement, Building and Environment, 241 (2023) 110486.

ACCEPTED MANUSCRIPT